European Commission

JRC TECHNICAL REPORTS

LWR Deputy: Electron probe micro-analysis of a high burnup (Th,Pu)O2 fuel section

Philipp Pöml
Stéphane Brémier
Jérôme Himbert
José Ignacio Tijero Cavia

2015

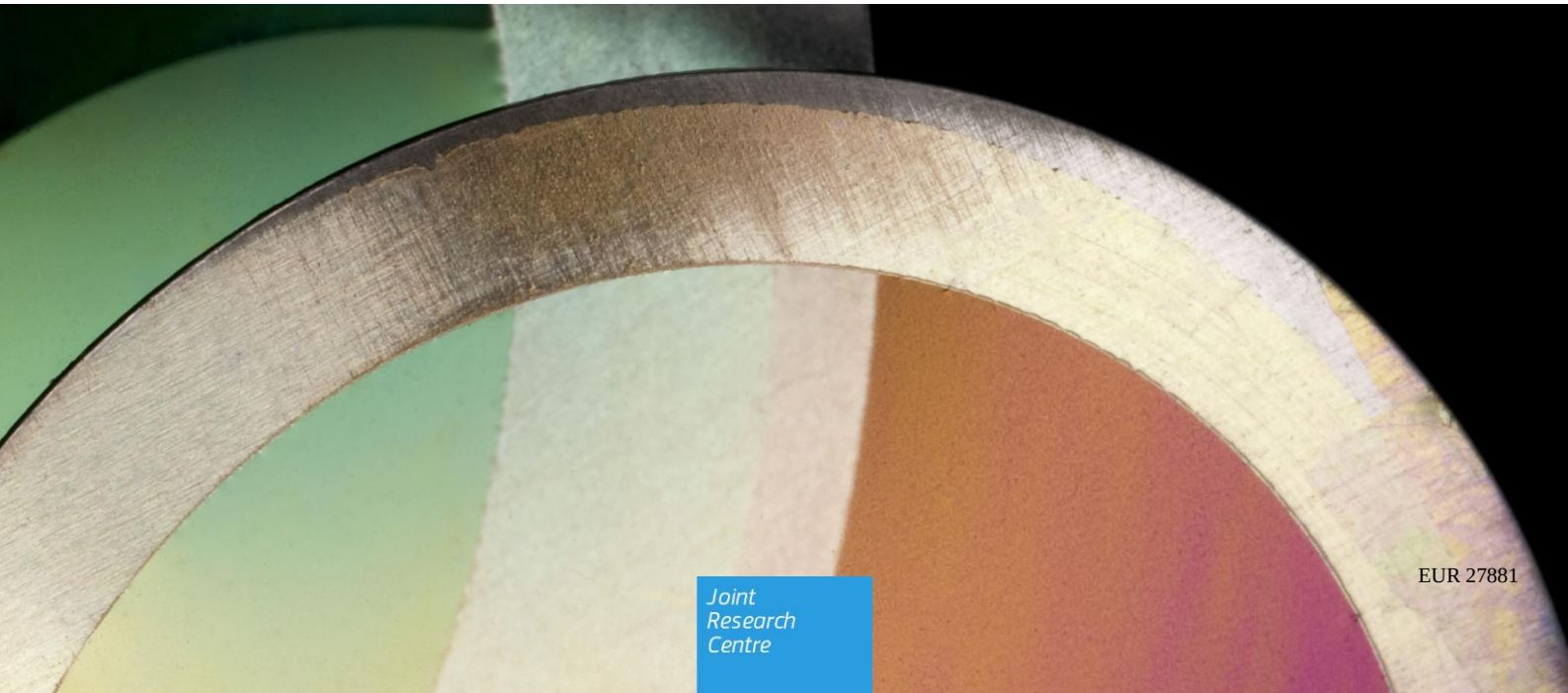

Joint Research Centre

EUR 27881

Contact information

Name: Philipp Pöml
Address: Hermann-von-Helmholtz-Platz 1, 76344 Eggenstein-Leopoldshafen
E-mail: philipp.poeml@ec.europa.eu
Tel.: +49-7247-951-867

JRC Science Hub
https://ec.europa.eu/jrc

JRC*98186*

EUR 27881-EN

ISBN 978-92-79-57863-2 (PDF)
ISBN 978-92-79-57862-5 (print)

ISSN 1831-9424 (online)
ISSN 1018-5593 (print)

doi:10.2789/272551 (online)
doi:10.2789/21583 (print)

How to cite: Philipp Pöml, Stéphane Brémier, Jérôme Himbert, José Ignacio Tijero Cavia; LWR Deputy: Electron probe micro-analysis of a high burnup (Th,Pu)O2 fuel section; EUR 27881; doi 10.2789/272551

Contents

List of Tables

List of Figures

Abstract

This report contains the results of electron probe microanalysis investigations on a high-burnup (Th,Pu)O2 fuel section. This work is done under the frame of the LWR Deputy programme. The work reports the concentrations of eight elements (Ru, Mo, Xe, Pu, Th, Cs, Nd, U) as a function of their radial distribution.

1 Introduction

This report contains the results of electron probe micro-analysis (EPMA) investigations on a high burn-up (38.8 MWd/kg HM) (Th,Pu)O_2 fuel section irradiated at KWO Obrigheim. The sample was KWO-Th-Pu-14, a 7 mm thick section taken from fuel rod KWO-TH-Pu-Rod-1 between pellets 11 and 12.

The work was done under the frame of the LWR Deputy programme (Light Water Reactor fuels for Deep Burning of Pu in Thermal Systems) funded by FP6-EURATOM-NUWASTE. The work was foreseen in work package 3 under topic 3.1: Post-irradiation examination. LWR-DEPUTY was conceived to fit in a portfolio of experimental research on novel fuels for deep burning of plutonium in existing nuclear power plants (NPPs).

The main objective of the work is to create an experimental database on the basis of which a benchmark modelling exercise could be defined. The focus lies on the actinide inventory of plutonium-thorium oxide fuel. It allows fuel modellers to test, validate and compare different calculation codes that are applied. A comparison of theoretical with experimental data should lead to a better understanding of the burn-up behaviour of (Th,Pu)O_2 fuels in Light Water Reactors. Such knowledge underpins the predictions of in-reactor performance of these fuels and has its impact on all related aspects (burn-up behaviour, safety issues, etc.).

2 Methods

2.1 Instrument

The EPMA at ITU is a state-of-the-art Cameca SX100. It is fully shielded for the analysis of irradiated fuel samples. The SX100 is equipped with four vertical spectrometers, two of which have quartz $10\bar{1}1$ crystals installed for the analysis of actinide elements.

2.2 Point Analysis

For EPMA, the specimen was polished and coated with a conductive layer of aluminium of about 20 nm in thickness to avoid charging effects.

The conditions used for the point analysis are given in Table 1. The counting time was 50 s for the peak and 20 s each for the negative and the positive background positions. The counting times and beam intensities (I_b) were adjusted during the standardization procedure to account for beam sensitive standards. The matrix correction was made using the Full PAP [1] option in the Probe for EPMA analysis software (www.probesoftware.com).

Xenon was analysed using the method of Walker [2] using Sb together with a correction factor as a standard for Xe. This gives the concentration of Xe dissolved in the fuel matrix and in intragranular bubbles smaller than about 0.1 μm. Since

the correction factors given in [2] were developed for and are applicable to an older instrument, i.e., a Cameca MS46, new correction factors for the SX100 at ITU were recently determined following the same approach [3]. The confidence interval on the measured Xe concentration at a significance level of 99% is about 5% relative at a concentration of 0.5 wt.% and 10-20% relative at 0.05 wt.%.

The point analysis of the sample was carried out on 41 spots along the radius of the fuel pellet. The radial direction was selected as crack-free as possible. The concentrations of the elements in the spots were calculated from the average of six analyses. The analysed radius of the sample is shown in Figure 1 (white line). The distance of the analysed spots from the sample's centre are given in Table 3 as the relative radius r/r_0.

2.3 Interference corrections

Line interferences were thoroughly studied before the analyses.

Since the U Mα_1 line is heavily overlapped by the Th Mβ_1 line, it was decided to measure the U Mβ_1 line. However, the U Mβ_1 line had to be corrected for interference with the Th Mγ_2 (M_3-N_4) line. The Xe Lα_1 line could not be used, because it overlaps with the Th M_2-N_4 line. Therefore, the Xe Lβ_1 line was used. Close to the Xe Lβ_1 line, however, is the U M_2-N_4 line. Considering the peak positions showed that those lines are 150 spectrometer units (≈ 0.01 Å) apart. Considering also the very low concentration of U in the sample, it was concluded that the consequence of this overlap is negligible. Additionaly, a spectrum was acquired (Figure 2) which shows no significant U M_2-N_4 intensity/overlap issues.

The possibility for the analysis of krypton was also evaluated. Since the concentration of Kr is usually even lower than the one of Xe, insignificant intensity can be expected. Spectra looking for the Kr Kα_1 2nd order line were acquired on the LiF and quartz crystals, but no significant peaks could be detected. The Kr Lα_1 line can be detected with a TAP (Thallium acid phthalate) crystal. The acquired spectrum showed, however, that this line is overlapped heavily by Th and U lines, hence, no Kr Lα_1 signal/peak could be detected.

2.4 Radial Element Profiles

The concentrations of the elements in wt.% were plotted against the relative radius, r/r_0. The profiles were then smoothed and integrated to determine the average integrated concentration of each element.

2.5 Imaging

The secondary electron (SE) image of the specimen (Figure 1) was acquired at an acceleration potential (E_0) of 25 kV. The beam current (I_b) was 5 nA.

3 Results

Figure 1 shows a SE image of the analysed fuel sample KWO-Th-Pu-14. The sample surface shows some porosity and cracks. The white line marks the radius analysed.

The results for each spot are compiled for the sample KWO-Th-Pu-14 in Table 3. The radial distributions of the elements were then plotted as concentration (wt.%) vs. relative radius (r/r_0) in Figures 3 to 10.

The measured profiles for the elements are in general flat only for the inner half of the radius ($r/r_0 = 0$–0.5) after which the profiles start to show either an increasing or decreasing trend.

Figure 8 shows the Nd distribution in sample KWO-Th-Pu-14. The fission product Nd is a very good indicator for the local burn-up, because it is immobile as it dissolves in the fuel matrix. The Nd profile shows a slight increase in concentration of about 0.33–0.38 wt.% up to a relative radius of about 0.8. Then the Nd concentration increases rapidly. The U and Xe concentrations increase in the same region as the Nd concentration (Figures 4, 9). This is consistent with the generally observed higher burn-up at the outer surface of LWR fuel pellets; in this case this is due to local neutron capture of ^{232}Th and subsequent formation of fissile ^{233}U. Xe is a fission product.

The Pu profile (Figure 10) shows an unusual behaviour at the sample edge. The profile decreases as expected for $r/r_0 = 0$–0.95, however it shows an apparent increase at the very surface of the pellet. Calculations with TRANSURANUS indicate that at very high burnups the Pu profile for this type of fuel would indeed show increasing values at the outer surface of the pellet. However, the burnup of this sample is probably not high enough to show such a trend. With the current EPMA data set it cannot be unequivocally concluded that the observed increasing Pu trend at the sample surface is real. To confirm or better determine the Pu concentration at the sample surface, more EPMA point analyses with improved spatial resolution and counting statistics are needed.

For the U profile the innermost two spots show slightly higher concentrations compared to the neighbouring spots.

Table 2 compares the measured average integrated fission product concentrations with the expected fission product concentrations calculated from the burn-up and the fission yields. The burn-up was calculated from the measured Nd concentration considering the fission yields produced by U-233, U-235, Pu-239 and Pu-241. The contribution of each fission yield to the total fission yield was estimated by means of SERPENT and TRANSURANUS simulations . The initial fractions used for the calculation of the expected fission product concentrations were U-233 37.62 %, U-235 0.436 %, Pu-239 43.015 %, and Pu-241 18.929 %. The fission yields were taken from the JEFF-3.1 database (https://www.oecd-nea.org/dbforms/data/eva/evatapes/jeff_31/) apart from the value for Ru-99 produced by the fission of U-233, where the value of the JEFF-2.2 database was used, as the value in the JEFF-3.1 database seemed to be erroneous (four orders of mag-

nitude off), while the JEFF-2.2 value agreed with the values of the JENDL-3.2 and ENDF/B-VI databases.

Generally, the calculated and measured values (Table 2) match within the analytical error of the EPMA measurements. The measured average concentration for Cs is, however, lower by 38 % than the calculated average concentration. The Cs profile being flat in the range of $r/r_0 = 0$–0.8 would indicate limited additional Cs release in the central (hot) part of the fuel pellet. Thus, a possible explanation for the overestimated fission yield of Cs could be the extremely high (i.e., the highest known one) thermal neutron cross section of Xe-135 ($\sigma = 2.65 \times 10^6$ barn). Almost all of the Cs-135 is produced by the decay of Xe-135, which has a high fission yield (7.63 % for Pu-239). Because of its extremely high thermal neutron capture cross section, however, Xe-135 will more likely capture a neutron than decay to Cs-135. Consequently, the fission yield for Cs-135 may be strongly overestimated, probably by some orders of magnitude. A recalculation of the expected Cs concentration taking into account only Cs-133 and Cs-137 gives a value of 0.26 wt. % Cs, which fits much better the experimental value of 0.24 wt. % Cs measured by EPMA. First simulations with the improved TRANSURANUS code (which takes into account the neutron capture of Xe-135) give an average for the Cs profile of ≈ 0.27 wt. %, which fits very well with the data presented here.

4 Summary and conclusions

The EPMA measurements on the sample were completed successfully. The distribution of eight elements have been determined as a function of their radial position.

References

[1] Pouchou J L and Pichoir F 1984 *Recherche Aérospatiale* 167–192

[2] Walker C T 1979 *Journal of Nuclear Materials* **80** 190–193

[3] Pöml P, Brémier S, Laheurte F, Hasnaoui R and Walker C T 2009 *IOP Conference Series: Materials Science and Engineering* **7**

Table 1: Conditions used for quantitative electron microprobe analysis.

Element	X-ray Line	Diffracting Crystal	E_0 (kV)	I_b (nA)	Standard
Ru	Lα_1	PET[a]	25	250	Ru
Mo	Lα_1	PET	25	250	Mo
Xe	Lβ_1	Quartz $10\bar{1}1$	25	250	Sb
Pu	Mβ_1	Quartz $10\bar{1}1$	25	250	PuO_2
Th	Mα_1	Quartz $10\bar{1}1$	25	250	ThO_2
Cs	Lα_1	LiF	25	250	Pollucite[b]
Nd	Lα_1	LiF	25	250	$NdPO_4$
U	Mβ_1	Quartz $10\bar{1}1$	25	250	UO_2

[a] PET = Pentaerythritol
[b] Pollucite = $(Cs,Na)_2Al_2Si_4O_{12} \cdot (H_2O)$

Table 2: Comparison of the expected fission product concentration calculated from the burn-up of the sample KWO-Th-Pu-14 and the concentrations derived from the EPMA analysis. For Cs two values are given, see chapter 3, paragraph 6.

Element	Calculated (produced) values, wt.%	Average integrated conc. from graph, wt.%
Xe	0.46	0.49
Cs	0.39[a]	0.24
	0.26[b]	
Mo	0.31	0.32
Ru	0.29	0.24
Nd	—	0.37

[a] calculated taking into account Cs-135
[b] calculated without Cs-135

Table 3: Electron microprobe analysis results for sample KWO-Th-Pu-14.

r/r_0	Ru	Mo	Xe	Pu	Th	Cs	Nd	U	O	Total
0.998	0.31	0.47	0.73	0.63	76.67	0.37	0.57	2.57	12.12	94.43
0.985	0.30	0.46	0.69	0.57	76.97	0.34	0.51	2.21	12.12	94.18
0.973	0.28	0.41	0.65	0.60	77.79	0.33	0.49	2.00	12.12	94.67
0.961	0.28	0.39	0.61	0.55	78.32	0.30	0.47	1.86	12.12	94.88
0.949	0.28	0.39	0.61	0.57	78.32	0.30	0.45	1.75	12.12	94.78
0.937	0.27	0.38	0.59	0.65	78.74	0.29	0.44	1.66	12.12	95.14
0.925	0.28	0.38	0.60	0.63	79.21	0.28	0.43	1.62	12.12	95.55
0.912	0.27	0.37	0.61	0.65	79.17	0.28	0.42	1.57	12.12	95.45
0.900	0.27	0.36	0.56	0.62	79.53	0.27	0.42	1.52	12.12	95.67
0.888	0.26	0.35	0.55	0.64	79.23	0.27	0.42	1.52	12.12	95.37
0.864	0.26	0.35	0.55	0.67	80.33	0.27	0.40	1.45	12.12	96.40
0.839	0.25	0.34	0.52	0.65	79.95	0.26	0.39	1.39	12.12	95.86
0.815	0.26	0.35	0.51	0.66	79.74	0.25	0.38	1.34	12.12	95.61
0.791	0.25	0.32	0.52	0.74	79.48	0.25	0.38	1.31	12.12	95.36
0.766	0.25	0.34	0.53	0.68	79.61	0.26	0.38	1.31	12.12	95.47
0.742	0.25	0.32	0.51	0.71	79.64	0.25	0.37	1.26	12.12	95.42
0.718	0.24	0.33	0.50	0.70	79.84	0.25	0.37	1.24	12.12	95.58
0.693	0.24	0.33	0.50	0.69	79.88	0.24	0.37	1.24	12.12	95.62
0.669	0.24	0.33	0.49	0.71	79.50	0.25	0.36	1.18	12.12	95.17
0.645	0.23	0.33	0.49	0.73	79.88	0.24	0.36	1.21	12.12	95.60
0.620	0.24	0.33	0.49	0.72	79.81	0.24	0.36	1.20	12.12	95.52
0.596	0.24	0.32	0.48	0.76	79.85	0.23	0.36	1.19	12.12	95.55
0.570	0.24	0.31	0.48	0.71	80.34	0.23	0.36	1.19	12.12	95.99
0.550	0.24	0.31	0.49	0.78	80.40	0.23	0.36	1.17	12.12	96.11
0.520	0.23	0.31	0.47	0.75	80.58	0.24	0.35	1.20	12.12	96.25
0.500	0.24	0.30	0.46	0.77	80.55	0.23	0.36	1.16	12.12	96.18
0.470	0.23	0.31	0.48	0.78	80.74	0.23	0.35	1.16	12.12	96.40
0.450	0.23	0.31	0.47	0.76	80.80	0.22	0.34	1.14	12.12	96.39
0.426	0.23	0.30	0.46	0.78	80.83	0.23	0.35	1.15	12.12	96.44
0.401	0.23	0.30	0.46	0.79	80.48	0.23	0.34	1.13	12.12	96.08
0.365	0.23	0.30	0.45	0.80	80.76	0.22	0.34	1.12	12.12	96.34
0.328	0.23	0.32	0.45	0.80	80.70	0.22	0.34	1.10	12.12	96.27
0.292	0.23	0.30	0.47	0.80	80.60	0.22	0.34	1.09	12.12	96.16
0.255	0.22	0.30	0.45	0.80	80.63	0.22	0.34	1.08	12.12	96.17
0.219	0.23	0.29	0.46	0.81	80.69	0.22	0.35	1.08	12.12	96.25
0.182	0.23	0.29	0.46	0.80	80.58	0.22	0.33	1.09	12.12	96.12
0.146	0.23	0.30	0.45	0.80	80.58	0.22	0.33	1.07	12.12	96.09
0.109	0.23	0.29	0.47	0.85	80.56	0.22	0.33	1.08	12.12	96.15
0.073	0.23	0.30	0.45	0.79	80.65	0.22	0.34	1.06	12.12	96.15
0.036	0.22	0.30	0.47	0.82	80.05	0.24	0.33	1.17	12.12	95.72
0.000	0.22	0.29	0.45	0.82	80.08	0.23	0.33	1.16	12.12	95.70

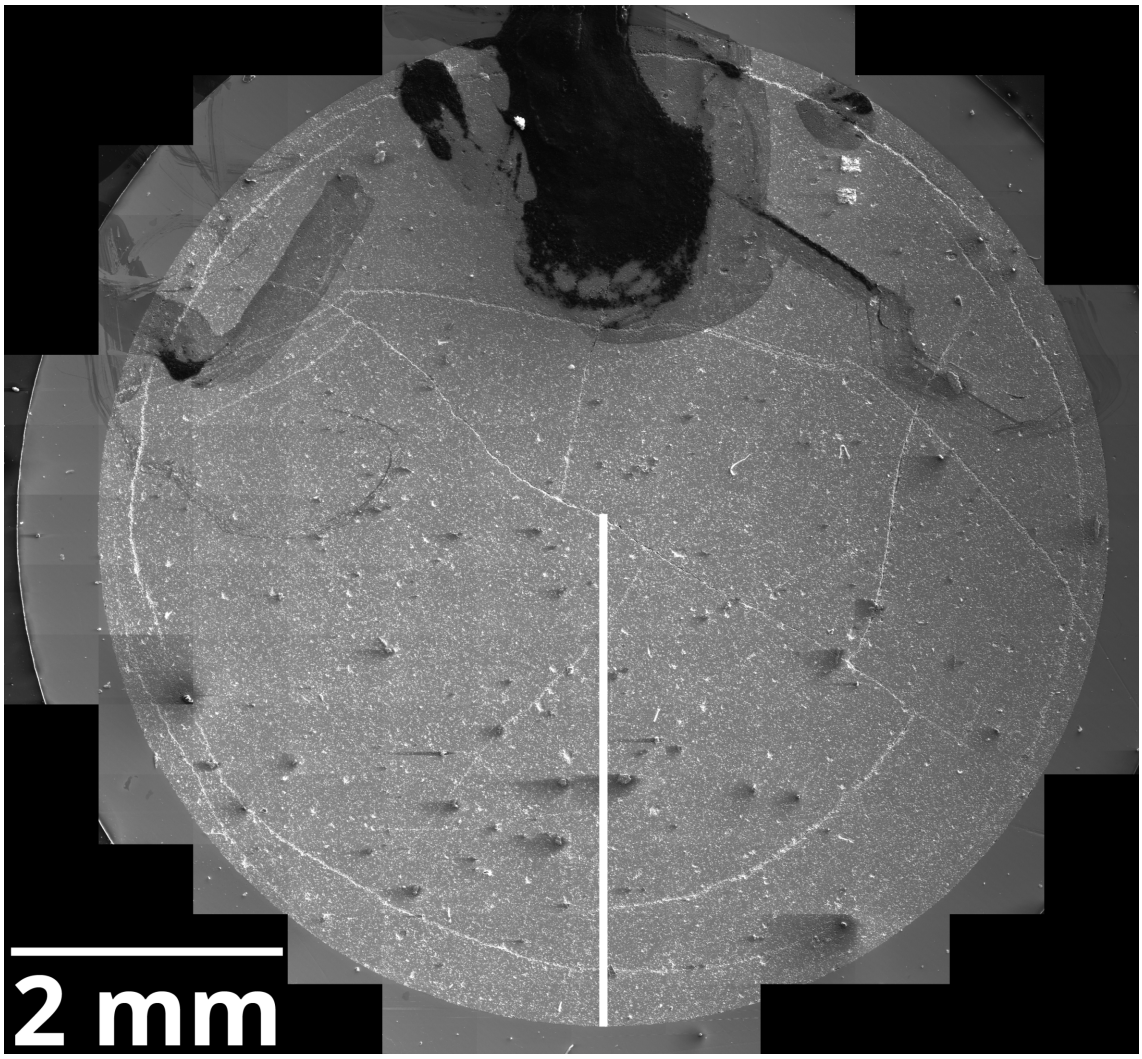

Figure 1: Secondary electron image of sample KWO-Th-Pu-14. The white line marks the analysed radius.

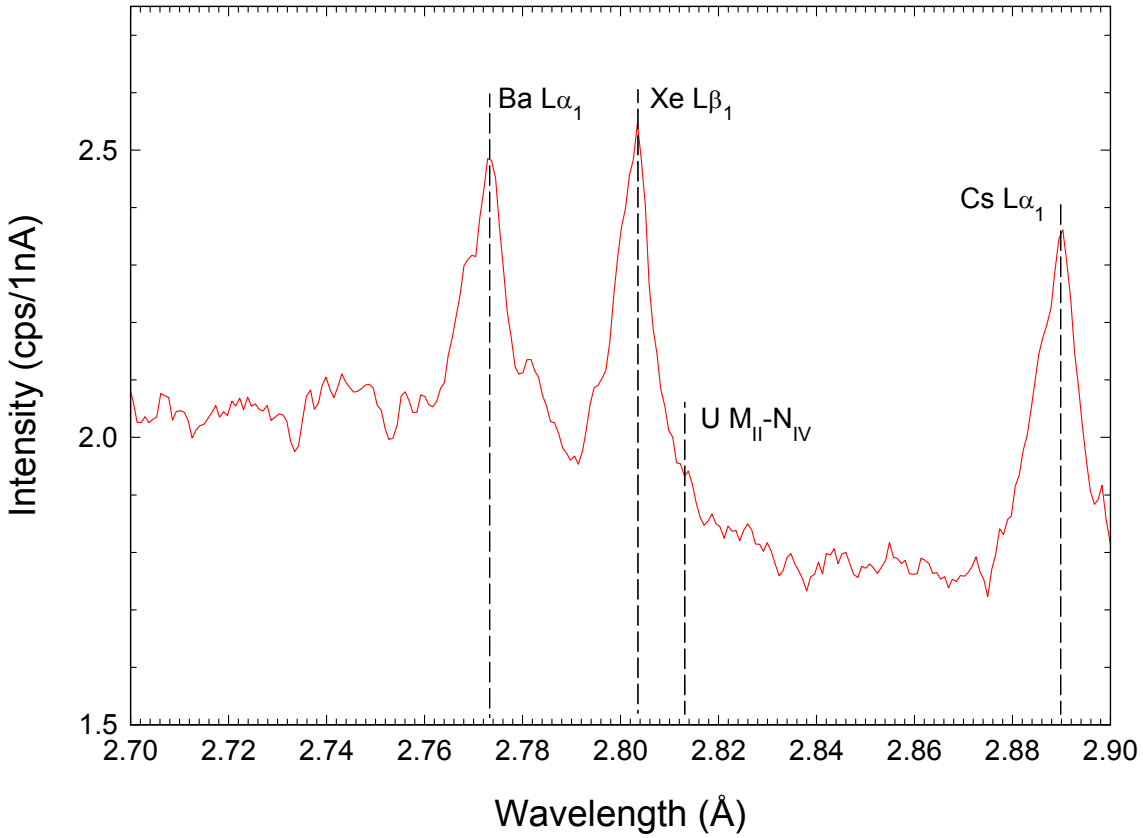

Figure 2: Spectrum of the quartz crystal between 2.7 and 2.9 Å taken on the edge of the fuel sample. The spectrum shows that the overlap of the U M_2-N_4 line on the Xe Lβ_1 line has a negligible effect. The peak of Ba Lα_1 shows that a significant amount of Ba is present in the sample. The Cs Lα_1 line is present at the low energy end of the spectrum.

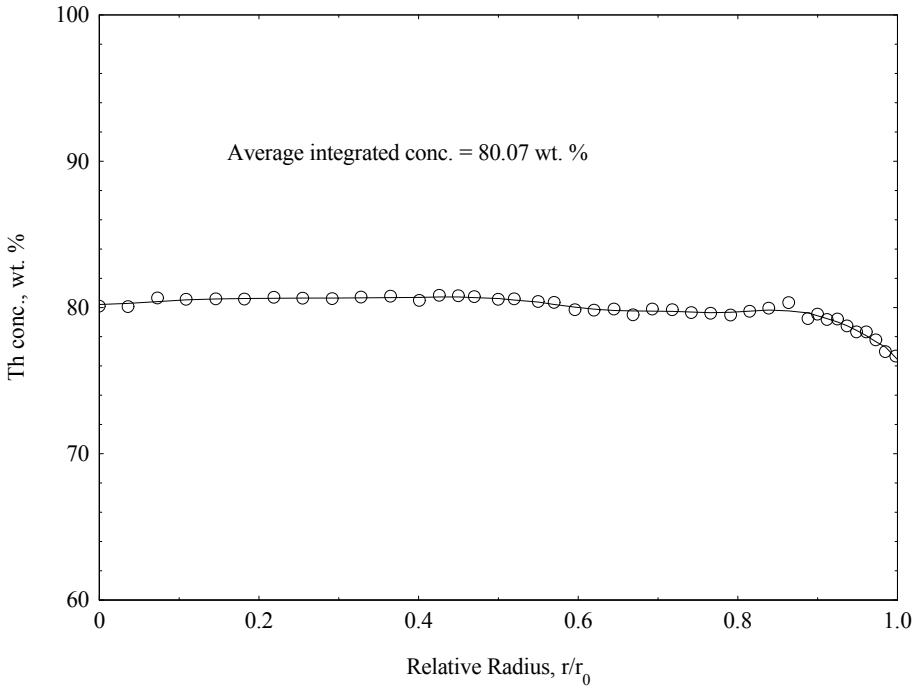

Figure 3: Radial distribution of Th in sample KWO-Th-Pu-14.

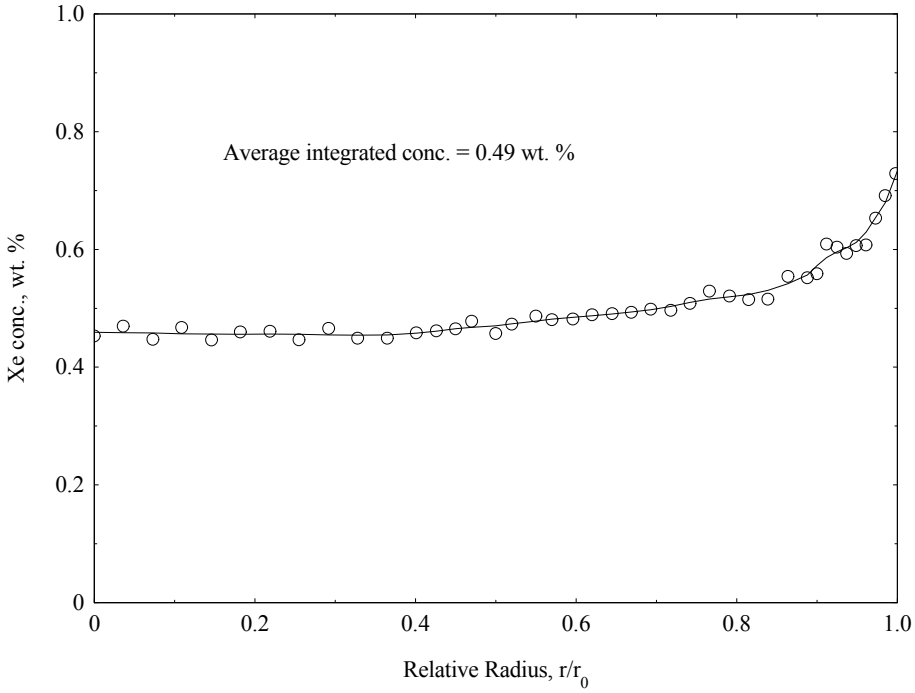

Figure 4: Radial distribution of Xe in sample KWO-Th-Pu-14.

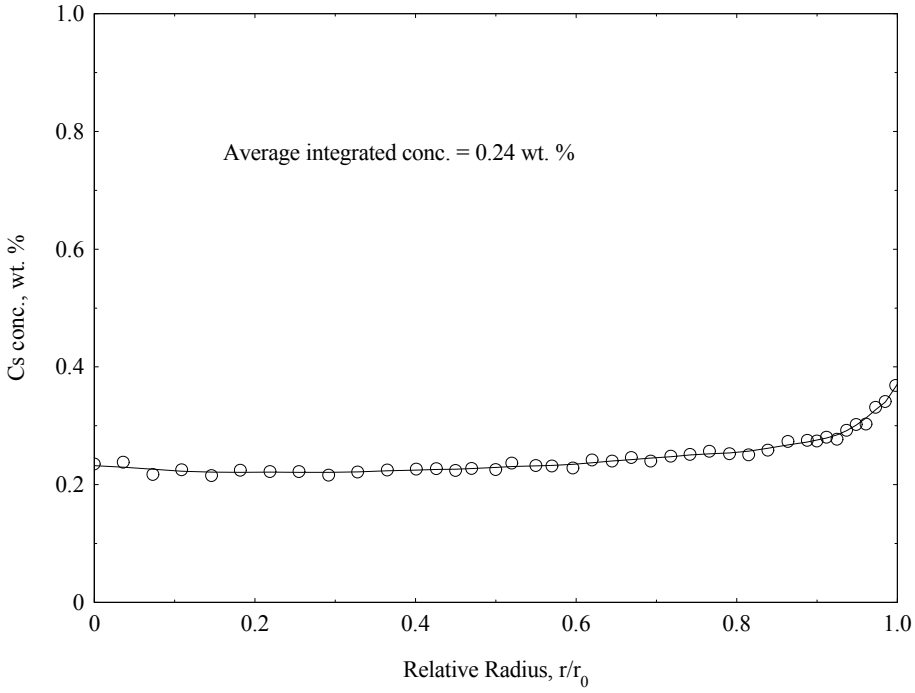

Figure 5: Radial distribution of Cs in sample KWO-Th-Pu-14.

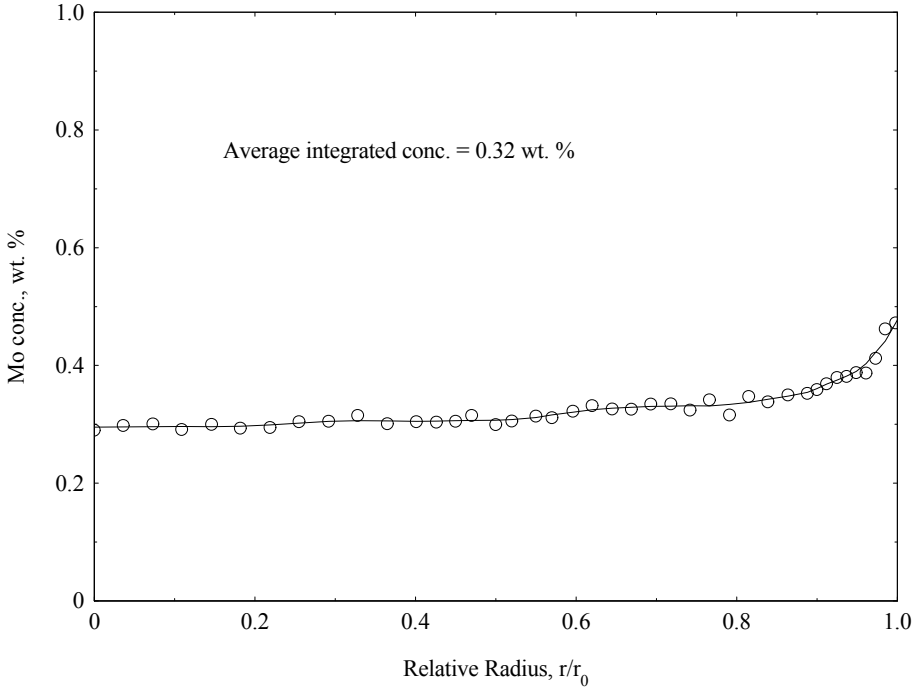

Figure 6: Radial distribution of Mo in sample KWO-Th-Pu-14.

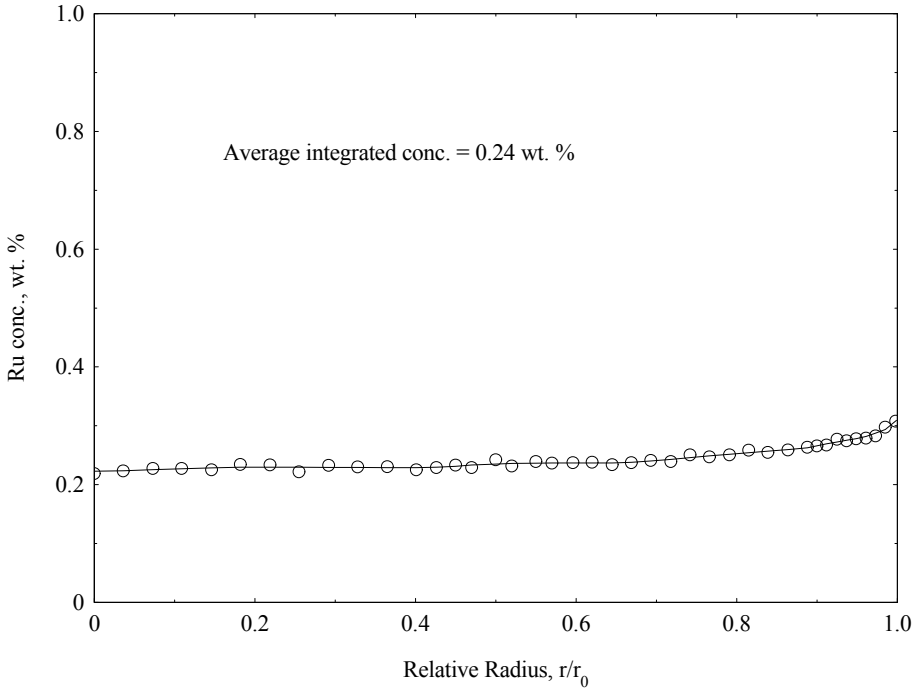

Figure 7: Radial distribution of Ru in sample KWO-Th-Pu-14.

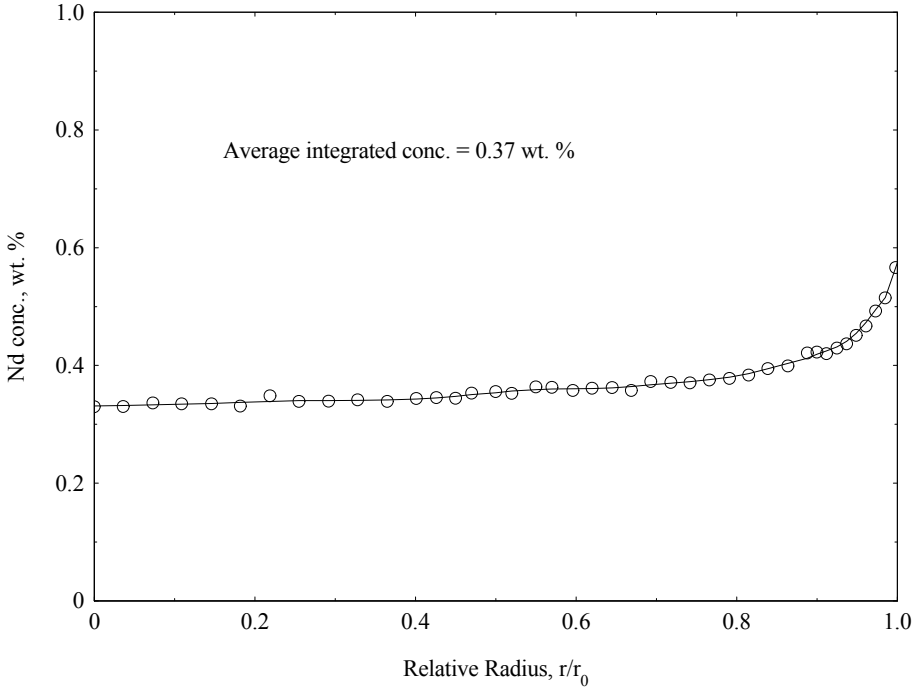

Figure 8: Radial distribution of Nd in sample KWO-Th-Pu-14.

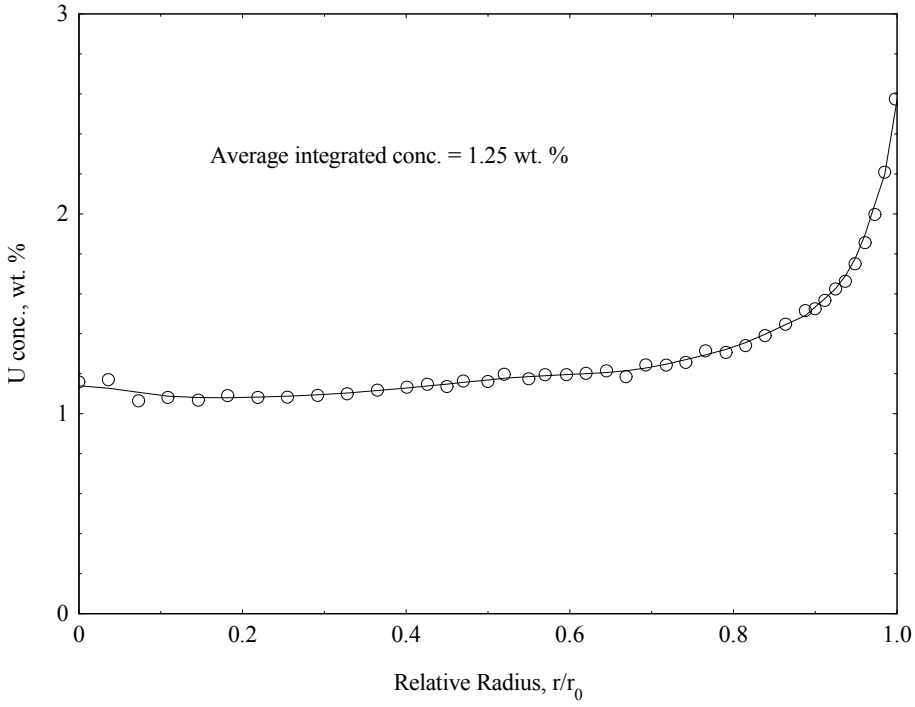

Figure 9: Radial distribution of U in sample KWO-Th-Pu-14.

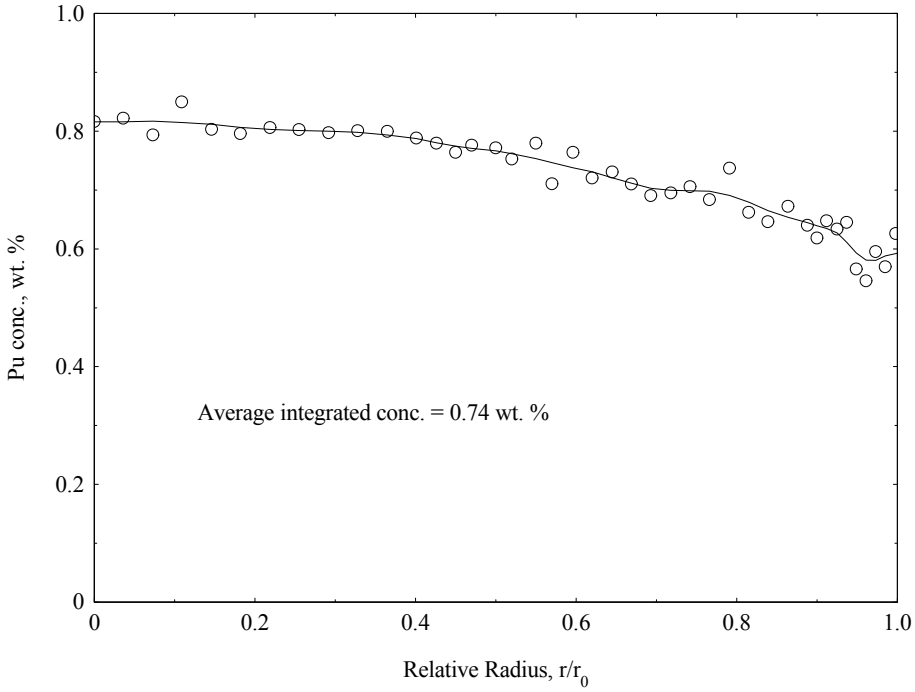

Figure 10: Radial distribution of Pu in sample KWO-Th-Pu-14.

Europe Direct is a service to help you find answers to your questions about the European Union
Free phone number (*): 00 800 6 7 8 9 10 11
(*) Certain mobile telephone operators do not allow access to 00 800 numbers or these calls may be billed.

A great deal of additional information on the European Union is available on the Internet.
It can be accessed through the Europa server http://europa.eu

How to obtain EU publications

Our publications are available from EU Bookshop (http://bookshop.europa.eu),
where you can place an order with the sales agent of your choice.

The Publications Office has a worldwide network of sales agents.
You can obtain their contact details by sending a fax to (352) 29 29-42758.

LC-NA-27881-EN-N

JRC Mission

As the Commission's in-house science service, the Joint Research Centre's mission is to provide EU policies with independent, evidence-based scientific and technical support throughout the whole policy cycle.

Working in close cooperation with policy Directorates-General, the JRC addresses key societal challenges while stimulating innovation through developing new methods, tools and standards, and sharing its know-how with the Member States, the scientific community and international partners.

Serving society
Stimulating innovation
Supporting legislation

doi:10.2789/272551

ISBN 978-92-79-57863-2